JOURNAL OF AIRCRAFT
Vol. 35, No. 4, July–August 1998

Simulation of Helicopter Rotor-System Structural Damage, Blade Mistracking, Friction, and Freeplay

Ranjan Ganguli* and Inderjit Chopra†
University of Maryland, College Park, Maryland 20742
and
David J. Haas‡
U.S. Naval Air Warfare Center, Bethesda, Maryland 20084

Selected helicopter rotor faults are simulated by changes in stiffness, inertial, and aerodynamic properties of the damaged or mistracked blade(s). A rotor aeroelastic analysis based on finite elements in space and time and capable of modeling dissimilar blades is used to simulate the damaged rotor in forward flight. The various rotor faults modeled include chordwise imbalance, aerodynamic mistracking, localized cracks, distributed changes in blade stiffness properties modeling a stiffness defect and a manufacturing defect, friction and freeplay in the pitch-control system and the lag damper, and friction in the flap and lag hinge. Changes in blade tip response and rotor hub loads are identified for the selected faults and tables of rotor-system diagnostics are compiled.

Nomenclature

C_d, C_l, C_m = blade section drag, lift, and moment coefficient
C_T = thrust coefficient
C_ζ = lag damper constant
c_0 = section lift coefficient at zero lift angle
c_1 = section lift curve slope
D = damage intensity factor
EI_y = flap stiffness
EI_z = lag stiffness
F_{xH} = longitudinal hub force
F_{yH} = lateral hub force
F_{zH} = vertical hub force
F_ζ = lag damper load
$F_{\zeta s}$ = steady component of damper load
$F_{\zeta v}$ = vibratory component of damper load
F_ϕ = pitch link load
GJ = torsion stiffness
M_{xH} = rolling hub moment
M_{yH} = pitching hub moment
M_{ys} = steady component of bending moment
M_{yv} = vibratory component of bending moment
M_{zH} = yawing hub moment
N = number of spatial finite elements
N_b = number of blades
R = rotor radius
T = kinetic energy
U = strain energy
v = lag deformation of blade
W = virtual work
w = flap deformation of blade
x = blade spanwise location of crack
α = angle of attack
Δ = difference between damaged and undamaged quantity
δ = variation
θ_0 = collective pitch
θ_{1c}, θ_{1s} = cyclic pitch
μ = advance ratio
σ = solidity ratio
ϕ = torsional deformation of blade
ψ = azimuth angle
Ω = rotation speed
ω = blade rotating frequencies
$\angle$ = change in phase angle

Subscripts
c = crack related quantity
d = damaged quantity
F = fuselage quantity, flap mode
R = rotor quantity
s = point of onset of freeplay
T = torsion mode
u = undamaged quantity

Superscripts
ic = ith sine component
is = ith sine component
NR = nonrotating quantity

Received Nov. 25, 1995; revision received Jan. 1, 1998; accepted for publication Jan. 9, 1998.

*Assistant Research Scientist, Alfred Gessow Rotorcraft Center, Department of Aerospace Engineering; currently Senior Engineer, Pratt and Whitney Aircraft, United Technologies Corporation, East Hartford, CT 06108. Member AIAA.

†Professor and Director, Alfred Gessow Rotorcraft Center, Department of Aerospace Engineering. Fellow AIAA.

‡Aerospace Engineer, Sea Based Aviation Office. Senior Member AIAA.

Introduction

THE helicopter rotor operates in a highly dynamic and unsteady aerodynamic environment leading to severe vibratory and fatigue loads on many critical components within the engine, transmission, drive shaft, and rotor system. Repeated exposure to this severe loading condition can induce damage in critical structural components, which, if unchecked, could lead to failure. To address this problem, damage-sensitive parts are frequently inspected and often prematurely replaced. This leads to higher operating and maintenance costs. In addition, excessive downtime of helicopters for inspection and maintenance may reduce availability and even jeopardize the mission. The need for a sizable reduction in the operating costs and for enhancement of flight reliability has directed attention to the development of rotorcraft health-monitoring systems. In this paper a mathematical model of the rotor system is used to

examine the system response of the helicopter as a result of selected rotor faults.

With regard to helicopter rotor systems, only limited work on damage simulation has been reported in the literature.[1] Azzam and Andrew[1] worked on the development of health and usage monitoring systems (HUMS) for helicopter rotors using computer-based mathematical models. Rotor-system faults were simulated for a five-bladed articulated rotor similar to the S-61 rotor. Faults modeled include blade cracks, chordwise mass imbalance, and defective lag damper. Selected validation of damaged rotor response and hub loads are presented. The present authors[2] formulated a damage-detection methodology for helicopter rotors. The rotor faults modeled were moisture absorption, loss of trim mass, damaged pitch-control system, misadjusted pitch link, damaged flap, and damaged lag damper. The influence of the simulated faults on blade response and hub loads was analyzed. Results from the study were summarized in the form of diagnostic tables that can be used by pattern recognition algorithms to detect damage.

In addition to helicopter rotor-system faults, rotor track and balance problems are also encountered by helicopter maintenance engineers. Rotor track and balance problems are caused by differences between blades that may be present because of manufacturing defects or misadjustments in mounting the blades on the hub. Track and balance problems cause changes in rotor-system behavior, which typically show up as an increase in fuselage vibration. Hub and blade balance weights, trim tabs, and pitch-link adjustments are used to correct rotor track and balance problems. Rotor aeroelastic analysis of dissimilar blades provides the means to compare various track and balance problems and determine the changes in rotor-system behavior caused by blade mistrack and blade damage. This is necessary for the health-monitoring system to differentiate between a mistracked or unbalanced rotor and a damaged rotor.

In contrast to the limited work on health monitoring of helicopter rotors, there has been considerable work in the areas of machinery diagnostics and space structures. The damage-detection techniques developed for machinery condition monitoring and space structures can serve as a guide for the more complex helicopter rotor-system damage-detection problem.

Potential faults in rotating machinery include shaft cracks, shaft imbalance, misalignment, rotor-to-stator rubbing, loose stationary and rotating parts, poorly lubricated bearings, and internal friction.[3–5] The objective of these analyses is to diagnose the state of the machine to perform preventive maintenance. Monitoring the dynamic behavior of machinery requires transducers that measure acceleration, velocity, and displacement at judiciously selected locations. In some applications the transducers are mounted permanently and the signal is monitored continuously for on-line health assessment.

In addition to rotating machinery, another area of active research in fault detection is space structures. On-line health-monitoring systems of space structures is important because of their inaccessibility to ground personnel. Researchers in the space structures field have integrated vibration analysis with system identification algorithms to produce quantitative damage-detection methods.[6] A mathematical model of the undamaged structure, usually correlated with experimental data of the undamaged structure, is used to analyze the vibration response of the damaged structure. The location and extent of the structural damage is monitored through system identification of the vibratory response of the space structure during its service life. Modal parameters such as natural frequencies and mode shapes from a damaged structure can be related to the system mass and stiffness properties of the undamaged structure. Comparison of the mass and stiffness properties between the damaged and undamaged structure identifies the damage location and extent. The feasibility of identifying mode shapes, frequencies, and damping of space structures in an on-orbit environment has also been addressed.[7]

The damage-detection techniques developed in the fields of rotating machinery and space structures can serve as initial guidance for the more complex rotor-system damage-detection problems. Work on turbine rotors, for example, is not readily applicable to helicopter rotors because helicopter rotors have 1) flexible and articulated blades in flap and lag, 2) variable pitch, 3) limited number of blades (typically, two to five), 4) nonaxial aerodynamic environment, 5) rotation rate much less than turbine rotors, and 6) high added damping in the lag mode. Work on space structures is not readily applicable to helicopter rotors because rotors have 1) strong aeroelastic interactions, 2) highly flexible rotating blades leading to nonlinearities because of Coriolis forces and moderate deflections, 3) periodic nature of blade response, and 4) strong modal coupling between blade modes.

In the absence of a large database of damaged system response, a key component of a successful damage-detection algorithm is an accurate mathematical model, usually a finite element model, of the system under investigation. Over the past few years a comprehensive rotor aeroelastic analysis based on a finite element method is space and time has been developed with the capability to provide accurate and detailed analysis of a typical helicopter rotor system.[8] The analysis has been validated with experimental and flight-test data for a wide range of flight conditions and rotor configurations. A specialized feature of the analysis of direct relevance to damage detection is the capability to model dissimilar blades. This dissimilarity can be in terms of blade structural, inertial, and aerodynamic properties.

Formulation

Mathematical Model of Rotor System

The helicopter is represented by a nonlinear model of several elastic rotor blades dynamically coupled to a six-degree-of-freedom rigid fuselage. Each blade undergoes flap bending, lag bending, elastic twist and axial displacement. Formulation is based on a generalized Hamilton's principle applicable to nonconservative systems:

$$\int_{\psi_1}^{\psi_2} (\delta U - \delta T - \delta W)\, d\psi = 0 \tag{1}$$

The δU and δT include energy contributions from components that are attached to the blade, e.g., pitch link, lag damper, etc. External aerodynamic forces on the rotor blade contribute to the virtual work variational δW. For the aeroelastic analysis in this study aerodynamic forces and moments are calculated using free-wake and unsteady aerodynamics for the forward-flight condition. Compressibility effects are accounted using the Prandtl–Glauert correction factor for quasisteady aerodynamics and the Leishman–Beddoes unsteady model used in the study also inherently accounts for compressibility. Apparent mass effects are included for noncirculatory airloads, and reversed flow is also included in the aerodynamic model. Finite element methodology is used to discretize the governing equations of motion and allows for accurate representation of complex hub kinematics and nonuniform blade properties. Beam finite elements with 15 degrees of freedom are used. These degrees of freedom correspond to cubic variations in axial elastic and bending deflections (flap and lag), and quadratic variation in elastic torsion.

The first step in the aeroelastic analysis procedure is to trim the vehicle for the specified operating condition. The blade finite element equations are transformed to normal mode space for efficient solution of the blade response. The nonlinear, periodic, normal mode equations are then solved for steady response using a finite element in time method. Steady and vibratory components of the rotating frame blade loads, i.e., shear forces and bending/torsion moments, are calculated using the force summation method. In this approach blade aero-

dynamic and inertia forces are integrated directly over the length of the blade. Fixed frame hub loads are calculated by summing the contributions of individual blades. A coupled trim procedure is carried out to solve for the blade response, pilot input trim controls, and vehicle orientation, simultaneously. The coupled trim procedure is essential for elastic blades because elastic deflections play an important role in the steady net forces and moments generated by the rotor.

Modeling of Selected Rotor-System Faults

The faults modeled in this paper are shown in Table 1 and are discussed next. Engineering judgement is used to quantify each rotor fault.

1) *Blade crack*: Cracks in the rotor blade cause a local reduction in blade stiffness. A blade crack is simulated by reducing the stiffness of a small finite element of length 1% of the blade length:

$$EI_{yc} = (1 - D_F)EI_{y0}, \qquad EI_{zc} = (1 - D_L)EI_{z0}$$
$$GJ_c = (1 - D_T)GJ_0 \tag{2}$$

D ranges from zero for no crack to 1.0 for a complete crack. The subscripts F, L, and T refer to flap, lag, and torsion respectively. The value of D can be obtained from experiment or fracture mechanics models.[1] Using this approach the detailed description of a blade failure mode does not need to be considered; only the associated reduction in stiffness is implemented.

Reductions in flap, lag, and torsional stiffness are investigated separately. Four damage locations on the blade are considered: 1) blade root ($x = 0$), 2) 30% blade span ($x = 0.3$), 3) midpoint ($x = 0.5$), and 4) 70% blade span ($x = 0.7$). For each damage location the baseline finite element mesh shown in Fig. 1 is refined until the frequencies converge. Details about the frequencies of the cracked blade for various damage-intensity factors and for all the damage locations are given in Ref. 9.

The nonrotating lag, flap, and torsion frequencies are shown in Figs. 2a–2c, respectively. In these figures D is increased from 0 to 1 at the spanwise location $x = 0.3$. Observable changes in the nonrotating frequencies occur when $D > 0.5$. It is clear from these figures that a very large reduction in stiffness is required to cause measurable change in frequencies. This is because of the flexible nature of the rotor blade and the short length of the assumed crack (1% of blade span).

Table 1 Potential rotor head damage

Rotor fault	Simulation of damage
Chordwise imbalance	Shift in blade c.g. at damaged section
Track split	Damaged blade flaps higher than undamaged blade
Torsion crack	Reduction in blade torsion stiffness at crack location
Bending crack	Reduction in blade lag stiffness at crack location
Compound crack	Reduction in all blade stiffnesses at crack location
Stiffness defect	Reduction in all blade stiffnesses at damaged section
Manufacturing defect	Uniform reduction in all defective blade stiffnesses
Freeplay in pitch-control	Nonlinear spring
Freeplay in lag damper	Nonlinear damper
Friction in lag hinge	Coulomb damping
Friction in flap hinge	Coulomb damping
Friction in pitch-control	Coulomb damping

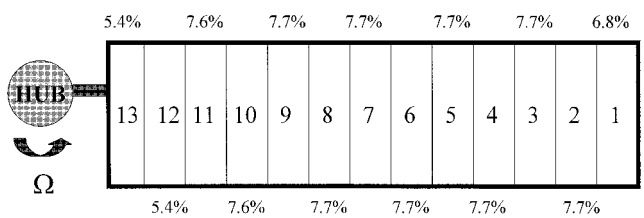

Fig. 1 Finite element model of baseline blade (element length shown as percent radius).

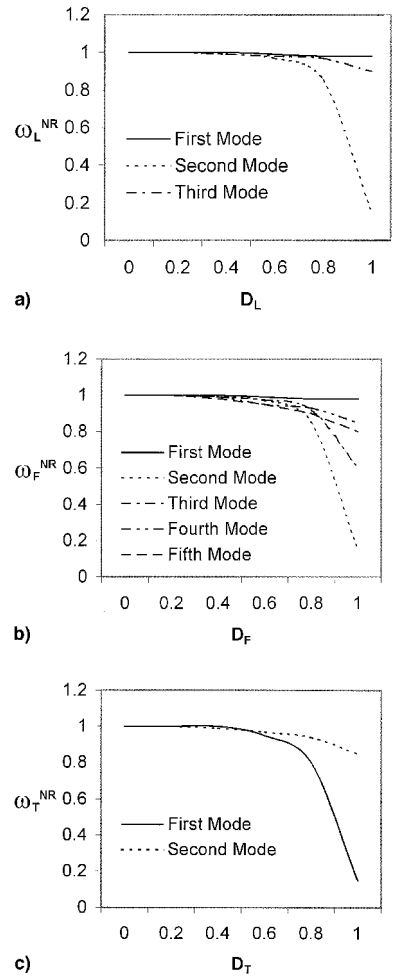

Fig. 2 Nonrotating a) lag, b) flap, and c) torsion frequencies with increasing damage intensity, normalized by baseline value.

For rotor-system response results in this paper three types of cracks are considered at the blade midspan ($x = 0.5$). The torsion crack is simulated by a reduction in GJ of 25%. The bending crack is simulated by a reduction in EI_z of 50%. The compound crack is simulated by a reduction in flap, lag, and torsion stiffness by 25%.

2) *Stiffness defect*: A stiffness defect is modeled as a reduction in blade stiffness over a larger area of the blade compared to a crack. Such a defect could arise from a structural flaw such as a growing crack or delamination. For simulation purposes the flap, lag, and torsion stiffness of the seventh element of the blade is reduced by 25% from the baseline value. This finite element is 7.7% of the blade length and is located at the midspan, as shown in Fig. 1.

3) *Manufacturing defect*: Because of manufacturing defects rotor blades may differ slightly in stiffness properties from one another. To simulate a manufacturing defect, the flap, lag, and torsion stiffness of the damaged blade is reduced by 3% over the entire blade span.

4) *Chordwise imbalance*: Balance weights are often used for correcting rotor track and balance problems. For example, Fig. 3 shows a blade with two balance weights of 1 lb each placed at the blade tip. One weight is located $0.2c$ ahead of the quarter chord and the other is $0.2c$ behind the quarter chord. Rotor

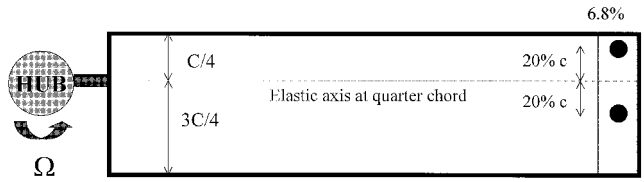

Fig. 3 Balance weights on blades used to correct track and balance problems.

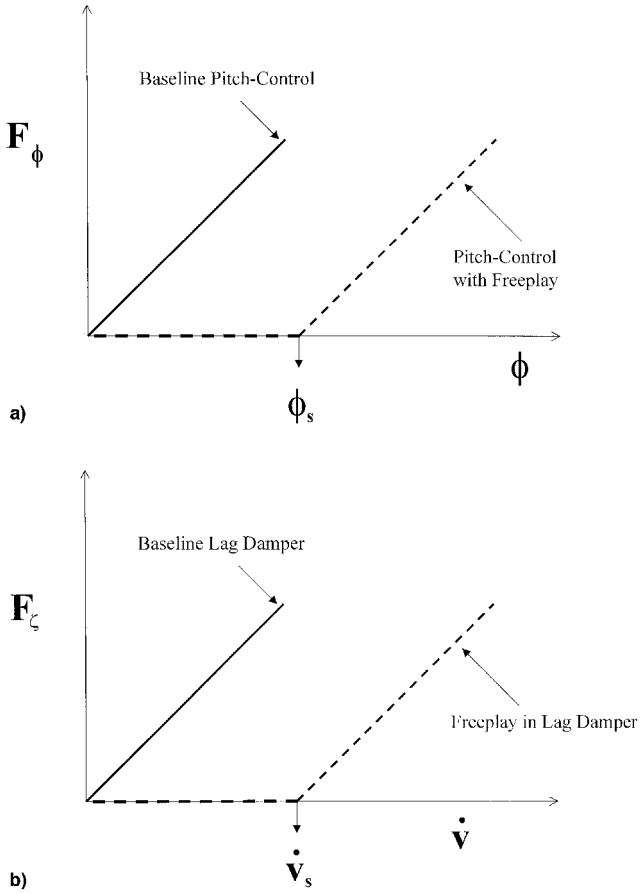

Fig. 4 Schematic representation of a) pitch-link and b) lag damper loads for blades with freeplay in pitch-control and lag damper, respectively.

balance problems can sometimes be corrected by redistributing these weights. To simulate chordwise imbalance the 1-lb weight is moved from the aft location to the forward location on the damaged blade. This results in the element c.g. moving ahead of the baseline position at the blade tip.

5) *Track split*: Track split is an example of aerodynamic mistracking where two opposite blades flap higher than the other two blades because of different pitch settings. By adjusting the pitch setting of some of the blades selected harmonics of the hub forces and moments can be reduced or eliminated. To simulate track split the pitch setting of the two opposite blades is increased by $\Delta\theta = 0.635$ deg such that the damaged blades flap 1.5 in. higher than the undamaged blades in hover ($\Delta w = 1.5$ in.).

6) *Freeplay in pitch control system*: The pitch-control system is exposed to severe loading conditions that can cause wear and looseness leading to freeplay. Freeplay in the pitch-control system is modeled by the nonlinear spring, whose characteristics are shown in Fig. 4a. For the undamaged blade, the pitch-link load varies linearly with displacement and the pitch-link stiffness is K_ϕ. However, for the blade with freeplay in the pitch-control system, the pitch-link stiffness is zero unless

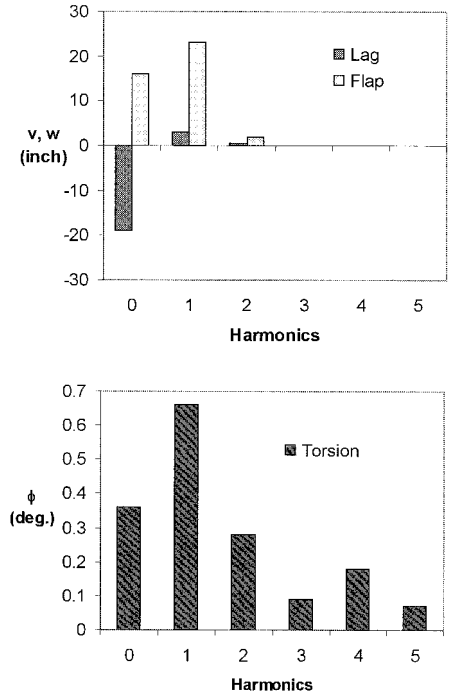

Fig. 5 Tip deflection for undamaged rotor blade.

the torsion displacement exceeds a value ϕ_s; thereafter the stiffness is K_ϕ

$$F_\phi = 0 \quad \text{for} \quad \phi < \phi_s$$
$$= K_\phi(\phi - \phi_s) \quad \text{for} \quad \phi \geq \phi_s \tag{3}$$

For numerical results ϕ_s of 0.15 deg is used. This is about half of the steady elastic twist of the undamaged blade (Fig. 5).

7) *Freeplay in lag damper*: The lag dampers used for articulated rotors are typically hydraulic dampers. These dampers have linear characteristics for most of their operating conditions. Sloppiness in the lag damper may cause the damper to lose its effectiveness at low values of lag velocity. This is modeled by the damper whose characteristics are shown in Fig. 4b. For the undamaged blade the damper load varies linearly with lag velocity and the damping value is C_ζ. However, for the blade with freeplay in the lag damper the damping is zero unless the lag velocity exceeds a value $\dot{v}_s$, thereafter the damping is C_ζ. In mathematical form the damper force is

$$F_{ld} = 0 \quad \text{for} \quad \dot{v} < \dot{v}_s$$
$$= C_\zeta(\dot{v} - \dot{v}_s) \quad \text{for} \quad \dot{v} \geq \dot{v}_s \tag{4}$$

For numerical results, $\dot{v}_s$ is equal to half the 1/rev lag velocity.

8) *Friction in hinges and bearings*: Coulomb friction damping is used to model friction at hinges or bearings caused by lack of lubrication or wear. The equations of motion for the baseline rotor blade without any friction damping can be written as

$$M\ddot{q} + C\dot{q} + Kq = F \tag{5}$$

When additional friction damping is added to the system the equations become

$$M\ddot{q} + C\dot{q} + \mu(\dot{q}/|\dot{q}|) + Kq = F \tag{6}$$

where μ is a measure of Coulomb friction damping in the system. Three cases are considered: 1) friction in the flap hinge, 2) friction in the lag hinge, and 3) friction in the pitch-

control system. For numerical results, a value of $\mu = 300$ is used.

Results and Discussion

Baseline Model

For results, a four-bladed articulated rotor with properties similar to a SH-60 helicopter is selected (see the following helicopter properties): rotor radius = 26.8 ft; flap and lag hinge offset = 15 in.; number of blades = 4; blade chord = 20.76 in.; linear aerodynamic twist = -18 deg; $C_l = 6.0\alpha$; $C_d = 0.002 + 0.2\alpha^2$; $C_m = 0.0$; lock number = 8.00; solidity = 0.0826; blade attachment point = 41.5 in.; rotor tip speed = 725 ft/s; helicopter weight = 16500 lb; and blade mass = 235 lb. The rotor blade is modeled using seven spatial finite elements along the blade span. Four-flap, two-lag, and one-torsion modes are used for analysis. Six-time finite elements with fourth-order shape functions are used along the azimuth to calculate the blade response. The results are obtained at a $C_T/\sigma = 0.0726$ at $\mu = 0.3$.

Selected predictions of component loads are compared with flight-test data. The flight-test data used consist of data collected during a flight loads survey of a highly instrumented SH-60B helicopter. During the flight-test program, parameters in the fixed system as well as component loads in the rotating system were measured. The component load data were sampled at a high rate and then filtered over each revolution of the rotor (one cycle) to extract minimum and maximum loads. From the minimum and maximum loads over each revolution, steady and vibratory components can be defined as

$$\text{Steady} = \frac{F_{\max} + F_{\min}}{2} \tag{7}$$

$$\text{Vibratory} = \frac{F_{\max} - F_{\min}}{2} \tag{8}$$

Results for the push rod loads are shown in Fig. 6. In this figure, the University of Maryland Advanced Rotorcraft Code predictions are compared with another aeroelastic analysis (CAMRAD/JA[10] as well as flight-test data. Bending moment at 15% span and lag damper load are compared with flight-test data in Figs. 7a and 7b, respectively. Prediction of helicopter loads is very dependent on aerodynamic modeling; the current study uses the Scully and Johnson free-wake model[11] and the Leishman and Beddoes unsteady aerodynamic model.[12] Both the flight test and analysis indicate the same trend with forward speed and an acceptable correlation between the analysis and flight-test data is obtained for the magnitudes of the steady and vibratory component loads.

Indicators of Rotor-System Damage

It is assumed that one blade is damaged and the other blades are undamaged. For the undamaged rotor (assuming perfectly tracked blades), all four blades will have identical tip response (magnitude and phase). Also, for a perfectly tracked rotor, only 4/rev and 8/rev forces and moments will be transmitted by the undamaged rotor to the fuselage.

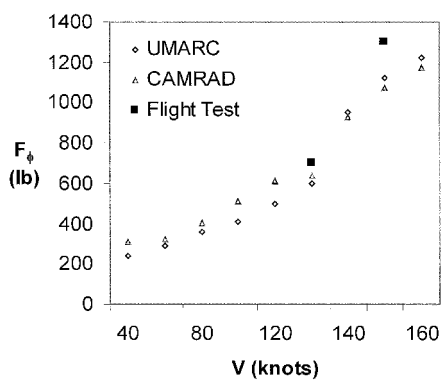

Fig. 6 Vibratory component of push-rod load.

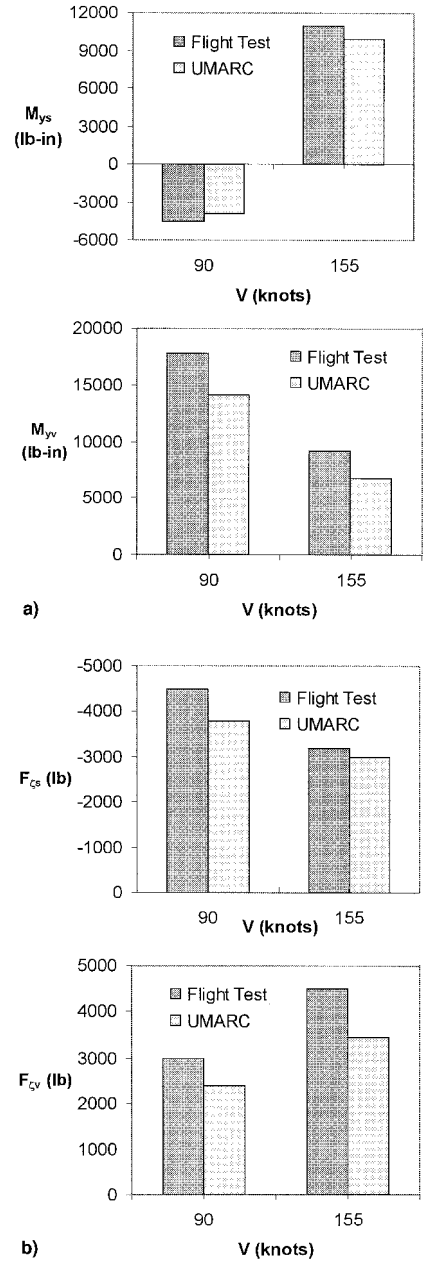

Fig. 7 Steady and vibratory component of a) bending moment at 15% blade span and b) damper load.

In practice, however, there will always be some level of fuselage response at 1/rev and at higher harmonics because of the inability to perfectly balance and track a rotor. Typically, a 1/rev fuselage response of 0.15 inch per second (ips), equivalent to about 170 lb, is representative of a well-balanced rotor. Vibrations in excess of 0.30 ips are considered significant and indicate the need to track and balance the rotor. Approximate thresholds for the moments transmitted to the fuselage can be similarly obtained. Moments below 2500 lb-in. are representative of a well-tracked and balanced rotor. Moments above 5000 lb-in. indicate the need to track and balance the rotor.

Similarly, for the blade tip response most real rotors display some degree of variation in tip displacements between blades, even when the rotor is considered to be in a tracked condition. In this study we assume that variations in tip deflections less than a quarter of an inch are negligible, and changes in elastic

twist of less than a quarter of a degree are considered too small to be of practical value. These measures for system response are shown in Table 2.

Forward-Flight Results

Results for the simulated damages are obtained in forward flight. The various damages listed in Table 1 are investigated separately. The baseline lag, flap, and torsion response for the undamaged rotor is shown in Fig. 5. The lag response is dominated by the steady component, whereas the flap response has a significant 1/rev harmonic component. Harmonics above 1/rev are negligible for the lag and flap response. The torsion response, however, has moderate higher harmonic component, including 1, 2, and 4/rev harmonics.

Rotor-System Diagnostics in Forward Flight

Tables 3–5 summarize the results obtained in this study in forward flight and provide a diagnostic feature map for each type of damage investigated. The symbols are defined in Table 2. Table 3 shows the change in the tip lag, flap, and torsion response in forward flight. The numbers in Table 3, next to the symbols, indicate the harmonics of the response. For example, 3-$\circ^+$, shows that the third harmonic is moderate and increases compared to the undamaged value. Tables 4 and 5 show the results for the hub forces and moments, respectively. Again, for example, 6-$\bigcirc$, indicates that the 6/rev component of the force harmonic is significant.

1) *Blade crack*: Local stiffness changes used to simulate a blade crack have negligible effect on the blade tip response. However, local changes in torsion stiffness of 25% at the blade midspan lead to a significant reduction in the 4/rev longitudinal force, a moderate reduction in the 4/rev vertical shear, and a significant increase in the 4/rev rolling moment. In addition, local change in the lag bending stiffness of 50% at the midspan result in a moderate change in the 4/rev lateral force and the 4/rev yawing moment. The rotor is least sensitive to local changes in flap stiffness and a change of over 90% is needed to cause moderate changes in rotor-system response. Therefore, a blade crack is most likely to change rotor-system behavior because of its influence on the local torsion stiffness.

2) *Stiffness defect and manufacturing defect*: Distributed reduction in blade stiffness representing stiffness and manufacturing defects cause moderate changes in steady flap and lag response, respectively. In addition, a moderate increase in the 4/rev vertical shear and the 4/rev yawing moment are produced.

3) *Chordwise imbalance*: Chordwise imbalance causes a significant change in the steady flap response and a moderate nose down 2/rev elastic twist. In addition, a significant reduction in the 4/rev vertical shear and a moderate increase in the 4/rev rolling and yawing moments are produced.

4) *Track split*: Track split causes a moderate reduction in the steady lag response and a significant increase in the steady flap response. In addition, a significant reduction in the 4/rev longitudinal force is produced. However, the distinguishing feature of track split is the significant 2/rev rolling and pitching moments.

5) *Freeplay in lag damper*: Freeplay in lag damper causes a moderate increase in the 1/rev elastic twist, a moderate change in the 4/rev lateral and vertical force and the 4/rev

Table 2 Quantitative measures for changes in system behavior

Degree of variation	Tip flap, lag, in. $\lvert\Delta w\rvert, \lvert\Delta v\rvert$	Tip torsion, deg $\lvert\Delta\phi\rvert$	Forces, lb $\lvert\Delta F\rvert$	Moments, lb-in. $\lvert\Delta M\rvert$	Phase, deg $\Delta\angle F$	Symbols
Negligible	<0.25	<0.25	<170	<2500	<10	~
Moderate	0.25–0.50	0.25–0.50	170–340	2500–5000	10–30	$\circ$
Significant	>0.50	>0.50	>340	>5000	>30	$\bigcirc$

Table 3 Rotor-system diagnostics in forward flight–blade tip response

Damage	Δv	$\angle v$	Δw	$\angle w$	$\Delta\phi$	$\angle\phi$
Chordwise imbalance	~	~	0-$\bigcirc^+$	~	2-$\circ^-$	2-$\circ^+$
Track split	0-$\circ^-$	~	0-$\bigcirc^+$	~	~	~
Torsion crack	~	~	~	~	~	~
Bending crack	~	~	~	~	~	~
Compound crack	~	~	~	~	~	~
Stiffness defect	~	~	0-$\circ^-$	~	~	~
Manufacturing defect	0-$\circ^+$	~	0-$\circ^-$	~	~	~
Freeplay in pitch-control	~	~	1-$\circ^+$	1-$\bigcirc^+$	2-$\circ^-$	~
Freeplay in lag damper	~	~	~	~	1-$\circ^+$	1-$\bigcirc^+$
Friction in lag hinge	2-$\circ^+$	2-$\circ^-$	1-$\circ^+$	~	1-$\circ^+$	~
Friction in flap hinge	2-$\circ^-$	2-$\bigcirc^+$	1-$\circ^+$, 2-$\circ^-$	~	1-$\circ^+$	~
Friction in pitch-control	2-$\circ^-$	2-$\circ^-$	0-$\circ^-$, 1-$\circ^-$	~	~	~

Table 4 Rotor-system diagnostics in forward flight–hub forces

Damage	$\lvert\Delta F_{xH}\rvert$	$\angle F_{xH}$	$\lvert\Delta F_{yH}\rvert$	$\angle F_{yH}$	$\lvert\Delta F_{zH}\rvert$	$\angle F_{zH}$
Chordwise imbalance	~	~	~	~	4-$\bigcirc^-$	~
Track split	4-$\bigcirc^-$	4-$\bigcirc^-$	~	~	~	~
Torsion crack	4-$\bigcirc^-$	4-$\circ^+$	~	~	4-$\circ^-$	4-$\circ^-$
Bending crack	~	~	4-$\circ^+$	4-$\circ^-$	~	~
Compound crack	4-$\bigcirc^-$	4-$\circ^+$	~	~	4-$\circ^+$	4-$\circ^-$
Stiffness defect	~	~	~	~	4-$\circ^+$	4-$\circ^-$
Manufacturing defect	~	~	~	~	4-$\circ^+$	4-$\circ^-$
Freeplay in pitch-control	~	~	1-$\circ^+$	1-$\bigcirc^+$	2-$\circ^-$	~
Freeplay in lag damper	~	~	~	~	1-$\circ^+$	1-$\bigcirc^+$
Friction in lag hinge	2-$\circ^+$	2-$\circ^-$	1-$\circ^+$	~	~	~
Friction in flap hinge	2-$\circ^-$	2-$\bigcirc^+$	1-2-$\circ^-$	~	1-$\circ^+$	~
Friction in pitch-control	2-$\circ^-$	2-$\circ^-$	0-1-$\circ^-$	~	~	~

Table 5 Rotor-system diagnostics in forward flight–hub moments

Damage	$\lvert\Delta M_{xH}\rvert$	$\angle M_{xH}$	$\lvert\Delta M_{yH}\rvert$	$\angle M_{yH}$	$\lvert\Delta M_{zH}\rvert$	$\angle M_{zH}$
Chordwise imbalance	4-o$^+$	4-o$^+$	~	~	4-o$^+$	4-o$^+$
Track split	2-◯$^+$	2-◯$^-$	2-◯$^+$	2-◯$^-$	~	~
Torsion crack	4-◯$^+$	4-o$^-$	~	~	~	~
Bending crack	~	~	~	~	4-o$^+$	4-o$^+$
Compound crack	4-◯$^+$	4-o$^-$	~	~	~	~
Stiffness defect	~	~	~	~	4-o$^+$	4-o$^-$
Manufacturing defect	~	~	~	~	4-o$^+$	4-o$^-$
Freeplay in pitch-control	4-o$^+$	4-o$^-$	4-o$^+$	4-o$^+$	~	~
Freeplay in lag damper	~	~	4-o$^+$	4-o$^+$	~	~
Friction in lag hinge	4-o$^+$	4-◯$^-$	~	~	~	~
Friction in flap hinge	4-o$^+$	4-◯$^+$	4-o$^+$	4-o$^-$	~	~
Friction in pitch-control	~	~	4-o$^+$	4-o$^-$	~	~

pitching moment, and a significant change in the 4/rev yaw moment.

6) *Freeplay in pitch-control system*: Freeplay in the pitch-control causes a moderate increase in the 1/rev flap deflection of the damaged blade and a moderate decrease in the 2/rev elastic twist. In addition, there is a moderate increase in the 4/rev rolling and pitching moment.

7) *Friction in lag hinge*: Friction in the lag hinge causes a moderate increase in the 2/rev lag response and the 1/rev flap response. In addition, there is a moderate reduction in the 4/rev vertical force and a moderate increase in the 4/rev rolling moment.

8) *Friction in flap hinge*: Friction in the flap hinge causes a moderate decrease in the 2/rev lag response, an increase in the 1/rev flap and torsion response, and a decrease in the 2/rev flap response. In addition, there is a moderate increase in the 4/rev longitudinal and vertical forces and a moderate increase in the 4/rev roll and pitch moments.

9) *Friction in pitch-control system*: Friction in the pitch-control system causes a moderate reduction in the 2/rev lag response and the steady and 1/rev flap response. In addition there is a moderate increase in the 4/rev longitudinal force and a significant increase in the 4/rev vertical force, and a moderate increase in the 4/rev pitch moment.

Conclusions

Selected rotor-system faults for a four-bladed articulated rotor similar to the SH-60 helicopter are modeled using a comprehensive aeroelastic analysis. Reasonable correlation between analytically predicted steady and vibratory rotor component loads and flight-test data is obtained for the undamaged rotor. The following conclusions are drawn by studying the changes in rotor-system behavior in forward flight.

1) *Blade crack*: Local stiffness changes used to simulate a blade crack have negligible influence on blade response and hub loads for low damage levels. Larger cracks causing local stiffness changes of over 50% can be detected by monitoring the 4/rev hub loads.

2) *Stiffness defect and manufacturing defect*: Distributed reduction in blade stiffness causing a stiffness defect and a manufacturing defect can be detected by monitoring the steady flap and lag response and the 4/rev hub loads.

3) *Chordwise imbalance*: Chordwise imbalance can be detected by monitoring the steady flap response, the 2/rev elastic twist, and the 4/rev hub loads.

4) *Track split*: Track split can de detected by monitoring the steady flap and lag response and the 2/rev and 4/rev hub loads.

5) *Freeplay*: Freeplay in the pitch-control system and the lag damper can be detected by monitoring the 1/rev flap response, the 1/rev and 2/rev torsion response of the damaged blade, and the 4/rev hub loads.

6) *Friction*: Friction in the flap and lag hinge and pitch-control system can be detected by monitoring the 2/rev lag response, steady, 1/rev and 2/rev flap response, 1/rev torsion response, and 4/rev hub loads.

Acknowledgments

This work was sponsored by the U.S. Naval Surface Warfare Center, Carderock Division. The Project Monitor was Wayne Boblitt.

References

[1]Azzam, H., and Andrew, M. J., "The Use of Math-Dynamic Models to Aid the Development of Integrated Health and Usage Monitoring Systems," *Journal of Aerospace Engineering*, Vol. 206, Pt. G, 1992, pp. 71–96.

[2]Ganguli, R., Chopra, I., and Haas, D. J., "Formulation of a Helicopter Rotor System Damage Detection Methodology," *Journal of the American Helicopter Society*, Vol. 41, No. 4, 1996, pp. 302–312.

[3]Kim, J. H., and Yang, W. J., *Dynamics of Rotating Machinery*, Hemisphere, New York, 1990, pp. 47–73.

[4]Mayes, I. W., and Davies, W. G. R., "Analysis of Response of a Multi-Rotor Bearing System Containing a Transverse Crack in a Rotor," *Journal of Vibration, Acoustics, Stress and Reliability in Design*, Vol. 106, No. 1, 1984, pp. 12–20.

[5]Grabowski, B., "The Vibrational Behavior of a Turbine Rotor Containing a Transverse Crack," *Journal of Mechanical Design*, Vol. 102, No. 1, 1979, pp. 18–24.

[6]Zimmerman, D. C., and Smith, S. W., "Model Refinement and Damage Location for Intelligent Structures," *Intelligent Structural Systems*, edited by H. S. Tzou and G. L. Anderson, Kluwer, Dordrecht, The Netherlands, 1992, pp. 44–61.

[7]Kim, H. M., and Doiron, H. H., "On-Orbit Modal Identification of Large Space Structures," *Sound and Vibration*, Vol. 26, No. 6, 1992, pp. 24–30.

[8]Bir, G., Chopra, I., Ganguli, R., Smith, E., "University of Maryland Advanced Rotorcraft Code Theory Manual," Univ. of Maryland, Aerospace Rept. 94-18, College Park, MD, July 1994.

[9]Ganguli, R., Chopra, I., and Haas, D. J., "Helicopter Rotor-System Damage Detection," *Proceedings of the Aeromechanics Specialist Meeting of the American Helicopter Society* (Fairfield County, CT), Oct. 1995, pp. 102–110.

[10]Johnson, W., "A Comprehensive Analytical Model of Rotorcraft Aerodynamics and Dynamics. Part 1: Analysis Development," NASA TM 811182, June 1980.

[11]Scully, M. P., "Computation of Helicopter Rotor Wake Geometry and Its Influence on Rotor Harmonic Airloads," Massachussetts Inst. of Technology, ASRL TR 178-1, Cambridge, MA, March 1975.

[12]Leishman, J. G., and Beddoes, T. S., "A Generalized Model for Unsteady Aerodynamic Behavior and Dynamic Stall using the Indicial Method," *Journal of the American Helicopter Society*, Vol. 36, No. 1, 1990, pp. 14–24.